Geomechanics and Engineering, *Vol. 17, No. 2 (2019) 157-164*
DOI: https://doi.org/10.12989/gae.2019.17.2.157

Change of pore structure and uniaxial compressive strength of sandstone under electrochemical coupling

Zhaoyun Chai*, Jinbo Bai and Yaohui Sun

Mining Technology Institute, Taiyuan University of Technology, Taiyuan, Shanxi 030024, China

(Received May 18, 2018, Revised January 7, 2019, Accepted January 10, 2019)

Abstract. The effect of electrochemical modification of the physical and mechanical properties of sandstone from Paleozoic coal measure strata was investigated by means of liquid nitrogen physical adsorption, X-ray diffraction and uniaxial compressive strength (UCS) tests using purified water, 1 mol/L NaCl, 1 mol/L $CaCl_2$ and 1 mol/L $AlCl_3$ aqueous solution as electrolytes. Electrochemical corrosion of electrodes and wire leads occurred mainly in the anodic zone. After electrochemical modification, pore morphology showed little change in distribution, decrease in total pore specific surface area and volume, and increased average pore diameter. The total pore specific surface area in the anodic zone was greater than in the cathodic zone, but total pore volume was less. Mineralogical composition was unchanged by the modification. Changes in UCS were caused by a number of factors, including corrosion, weakening by aqueous solutions, and electrochemical cementation, and electrochemical cementation stronger than corrosion and weakening by aqueous solutions.

Keywords: electrochemical coupling; pore structure; electrodes corrosion; physical and mechanical properties; Paleozoic sandstone

1. Introduction

The principles of electrochemical modification of rock or soil involve the application of a small direct current (DC) or a low potential gradient to electrodes inserted in the rock or soil mass. The transportation of charged species across the rock and soil mass involves several complex mechanisms such as electrolysis, electro-osmosis, electromigration and electrophoresis. This technique has been applied in geotechnical engineering for many decades (Casagrande 1952).

Pinzari (1962) modified the mudstone core in coal measure rocks using an electrochemical method, improving the tensile strength of the modified core by a factor of 3.3. Studies by Chilingar (1970) and Aggour *et al.* (1992, 1994) on the effects of DC on the permeability of sandstone and oil shale cores found that the permeability of both rock types increased with increasing electrical potential gradient. This appeared to be related to clay type and content, with smectite having the greatest effect, followed by illite, then kaolinite. Further studies have conclusively shown that changes occur in the crystal structures and that the interlamellar spacing of the rock minerals decreases when a current is passed through a core specimen. Bernabeu *et al.* (2001) studied the porosity of Bateig stone, and showed that electrochemical modification consolidated porous material, prevented decay and improved its resistance to water and weathering. Feijoo *et al.* (2017a, b, 2018) studied the physical and geomechanical properties of the granite, the results show that the electrokinetic treatment reduces the porosity of the rock, this porosity reduction lowers the entry and storage of external agents in the rock, and also increase its UCS, no mineralogical and aesthetic damages on the stone were detected after the treatment, confirming the reliability of this method to be applied in situ on granitic rocks.

Although such studies have demonstrated that the physical and mechanical properties of rock are improved by electrochemical modification, no reports of the application to the types of sandstone frequently encountered in underground coal mining operations and the effects of electrochemical modificaion have been published in geotechnical engineering contexts because little systematic study of the mechanisms, theory, methods, parameters and effects of applying electrochemical modification has been done. Therefore, the present study examined the influence of electrochemical modification on the electrodes and the mineralogical composition, pore structure and mechanical strength of sandstone. Analysis, observations and discussion of the test results follow.

2. Experimental method

2.1 Experimental specimen

The specimen, which was taken from the floor of No. 3 coal seam in the Yuwu mine, Shanxi Province, China, consisted of a continental facies lake sedimentary rock from the Paleozoic Permian Shanxi Formation. The bulk density of the sample was 2635 kg/m^3 and the moisture content was 1.35%. The mineralogical composition of the sample was analyzed quantitatively using an adiabatic method. The

*Corresponding author, Professor
E-mail: chaizhaoyun_2002@163.com

ISSN: 2005-307X (Print), 2092-6219 (Online)

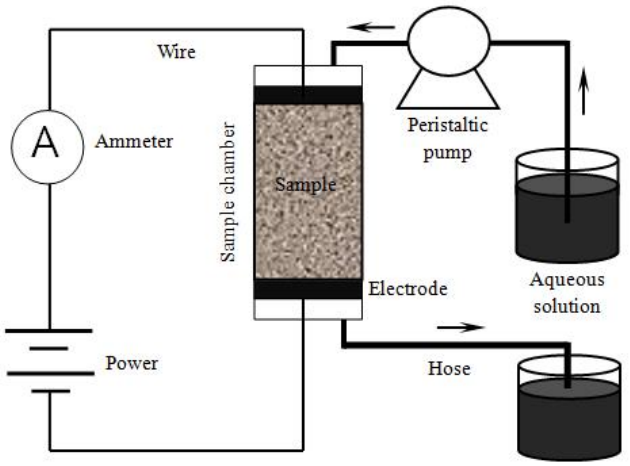

Fig. 1 Schematic of experimental apparatus

quartz, kaolinite, paragonite and zeolite contents in the sample were 70.34%, 23.48%, 3.06% and 3.13%, respectively. The specimen was sealed in the underground mine and processed into 20 cylindrical samples 50 mm diameter × 100 mm long in the laboratory, and then sealed with wax. Machining accuracy was strictly controlled, with adjacent perpendicular surfaces having a deviation less than 0.25° and opposite sides parallel at a deviation less than 0.05 mm.

2.2 Experimental apparatus

The experimental apparatus shown schematically in Fig. 1 consisted essentially of a DC power apply, ammeter, BT100-1J peristaltic pump, sample chamber, electrodes and solution tank. The sample chamber comprised an organic glass cylinder (wall thickness 5 mm × 50 mm i.d.) and piston, a circular porous plate and two electrodes. Thirteen 4 mm diameter holes (one central hole and 12 holes evenly distributed around the center) were drilled through the piston. A circular cavity 48 mm diameter × 5 mm deep was drilled into the top of piston to prevent the overflow of injected aqueous solution around the top edge. The circular porous plate was placed under the rock sample inside the cylinder. The electrodes consisted of 8 mm-thick circular steel plates with holes; the anode was placed on top of the sample, and the cathode under the sample. The DC output ranged from 0 to 110 V and up to 3 A, $\Phi 0.35 \times 1$ mm^2 silk-covered copper wire was used for the electrical wiring. The rotational speed of the pump was 0.1-10 rpm; the pump head was a YZ1515 model. The cross-section of the connecting hoses measured $\Phi 0.35 \times 2$ mm^2.

2.3 Experimental procedure

The outer circumferential surface of each test specimen was covered with a thin layer of petroleum jelly to minimize friction, then fitted snugly into the sample chamber. The power supply, ammeter and pump were then connected. The test specimens were initially at their natural moisture content. Four aqueous solutions (purified water, 1 mol/L NaCl, 1 mol/L $CaCl_2$ and 1 mol/L $AlCl_3$) were prepared for testing. The tests were carried out at room temperature (~23°C). The effect of any small fluctuations in temperature during the experiments was considered to be negligible.

The experimental procedure was (1) switch the pump on, and then (2) activate the power supply only after seepage of the pumped solution was visible from the bottom of the apparatus. (3) The flow rate of the pump was adjusted to ensure that the solution did not overflow from the cavity at the top of the piston. (4) The voltage gradient between the electrodes was maintained at 1 V per centimeter length of specimen. (5) After 96 h, the power supply was turned off and the specimen was removed from the chamber.

Uniaxial compression tests were then carried out in accordance with ISRM suggested methods. Three specimens were tested for each aqueous solution; the mean value was accepted as the test result in each case. After testing, the specimens were ground to a powder for X-ray diffraction pattern (XRD) and nitrogen adsorption isotherm analysis.

3. Results

3.1 Experimental observations

For salty aqueous solutions, white and locally faint blue salt crystals were formed at the wire/anode junction. When the insulation was stripped from the copper wire at the anode, the color of the wire was seen to have changed to black (Fig. 2); the wire to the cathode remained unchanged. This phenomenon is explained by electrophoresis: when an electric current is flowing, subject to space limitations, suspended micelles or colloidal particles migrate towards the anode and ultimately accumulate and separate out of the liquid around the junction of the wire and anode. At the same time, a layer of blue basic cupric carbonate ($Cu_2(OH)_2CO_3$) is generated on the surface of the copper wire in damp conditions. The blue and white precipitations mixed to form a white and local faint blue salt of crystallization. The blackening of the copper wire was caused by copper oxidation.

Fig. 2 Electrochemical corrosion of wire

(a) Anode (b) Cathode

Fig. 3 Corrosion state of electrodes

3.2 Electrode corrosion

The effect of applying a DC is to electrolyze water molecules, producing oxygen at the anode. Bubbles of oxygen were observed continually escaping from cavity in the top of piston into the liquid during the experiments. Reduction of the water at the cathode produced hydrogen. The reaction equations are

$$\text{Anodic zone: } 2H_2O - 2e^- \rightarrow O_2 \uparrow + 4H^+ \quad (1)$$

$$\text{Cathodic zone: } 2H_2O + 2e^- \rightarrow H_2 \uparrow + 2OH^- \quad (2)$$

However, when the aqueous solution is a chloride, electrolysis is composed of two steps. First, Cl^- ions are oxidized in the anodic zone producing chlorine, and the reduction of H^+ ions in the cathodic zone produces hydrogen. The reaction equations are

$$\text{Anodic zone: } 2Cl^- - 2e^- \rightarrow Cl_2 \uparrow \quad (3)$$

$$\text{Cathodic zone: } 2H^+ + 2e^- \rightarrow H_2 \uparrow \quad (4)$$

Thus, when Cl^- ions in the solution are exhausted, the reaction takes place according to Eqs. (1) and (2). Electrolysis alters the pH around the electrodes, decreasing around the anode (more acidic), and oxidizes and corrodes the anode. The pH increases around the cathode (more alkaline) such that it is not affected by corrosion (Fig. 3).

3.3 Pore structure changes

The test results for average pore diameter, accumulated pore specific surface area and volume of specimens from different zones before and after modification are shown in Table 1. Fig. 4 shows the relationship between pore diameter and specific surface area. Fig. 5 illustrates the relationship between pore diameter and volume. The following are clear from these curves.

(1) The pore diameter was concentrated in the ranges 3-5 nm (the lattice spacing of the clay minerals) and 20-40 nm, which represents the porosity of the skeleton particles of the sample.

(2) The pore morphology of the modified samples showed little change in distribution, but the total number of pores was significantly reduced, more so in the 3-5 nm range than in the 20-40 nm range.

(3) The total pore specific surface area of the modified samples was much less than in the original material in both the anodic zone (reduced to 53.4%-64.5%) and cathodic zone (reduced to 64.3%-70%) (Fig. 6). The total pore volume was reduced to 44%-53.2% in the anodic zone and 65%-84.8% in the cathodic zone (Fig. 6).

(4) The average pore diameter of the modified samples was greater than in the original, more so at the cathode than at the anode. Fig. 7 shows that the trend of the average pore diameter was 1 mol/L $AlCl_3$ < purified water < 1 mol/L NaCl < 1 mol/L $CaCl_2$ for the modified samples.

(5) The total pore specific surface area of the modified samples in the anodic zone was greater than in the cathodic zone; the total pore volume in the anodic zone was less than in the cathodic zone (Fig. 6). That is, fewer micro-pores were present in the anodic zone of the modified specimens

Table 1 Average pore diameter, specific surface area and volume in rock sample

Sampling area	Average pore diameter (/nm)	Accumulated pore specific surface area ($/m^2 \cdot g^{-1}$)	Accumulated pore volume ($/mm^3 \cdot g^{-1}$)
Original	12.38	8.95	27.7
Purified water anode	15.06	4.78	18.0
Purified water cathode	17.65	4.76	21.0
NaCl anode	16.87	5.29	17.8
NaCl cathode	17.77	4.22	23.5
$CaCl_2$ anode	18.33	4.80	19.4
$CaCl_2$ cathode	19.70	3.94	22.0
$AlCl_3$ anode	13.73	5.77	18.2
$AlCl_3$ anode	15.66	4.65	19.8

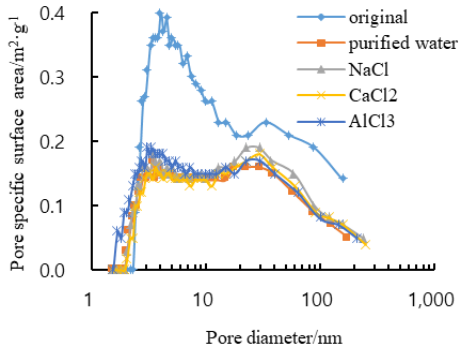

(a) Anodic zone

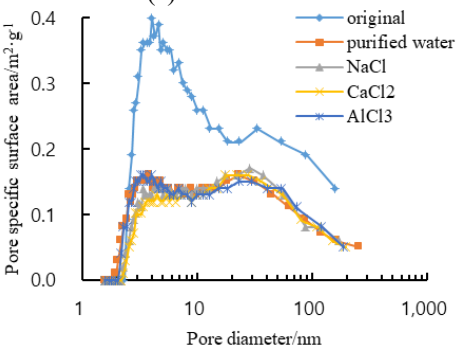

(b) Cathodic zone

Fig. 4 Pore specific surface area vs. pore diameter in different zones pre- and post-modification

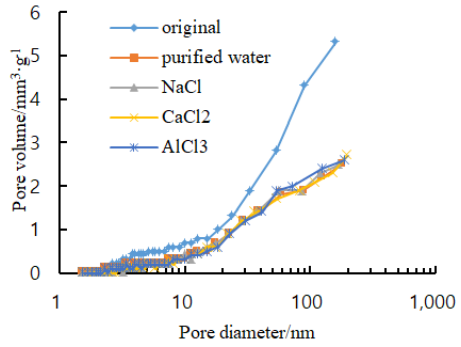

(a) Anodic zone

Fig. 5 Pore volume vs. pore diameter in different zones pre- and post- modification

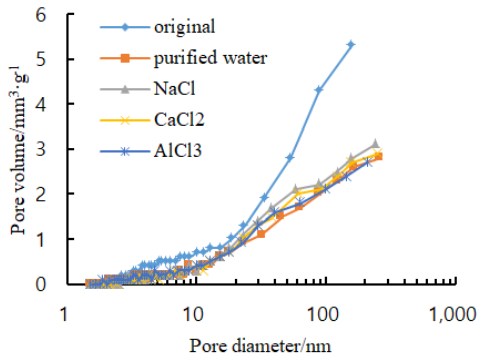

(b) Cathodic zone

Fig. 5 Continued

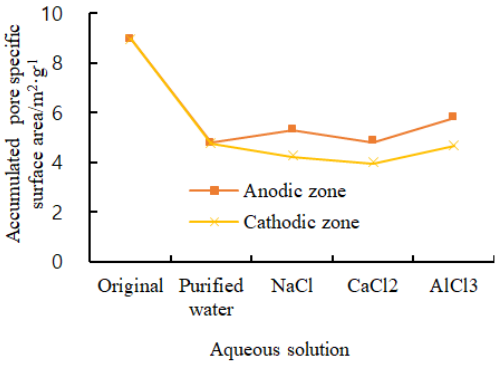

(a) Accumulated pore specific surface area

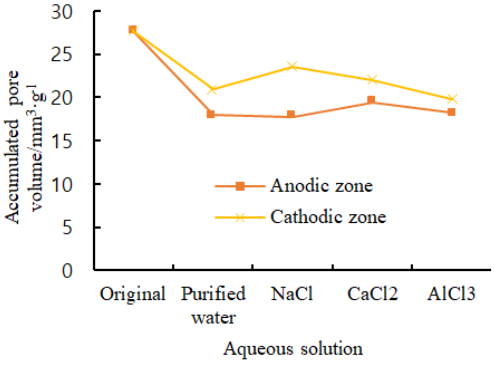

(b) Accumulated pore volume

Fig. 6 Accumulated pore specific surface area and pore volume of modified specimens for different electrochemical aqueous solutions

than in the cathodic zone, with correspondingly fewer meso-pores in the anodic zone than in the cathodic zone. This difference was caused by the electrokinetic effect of sandstone (Chai *et al.* 2016).

3.4 Mineralogical composition changes

Fig. 8 shows the XRD patterns for the specimens; Fig. 9 shows histograms of their mineralogical composition distribution. As shown, no new mineral was detected in samples from either the anodic or cathodic zone after modification by the aqueous solutions used in this study. The mineralogical composition also remained unchanged: quartz 70±5%, kaolinite 20 ± 5%, paragonite 4 ± 1% and zeolite 3 ± 1%.

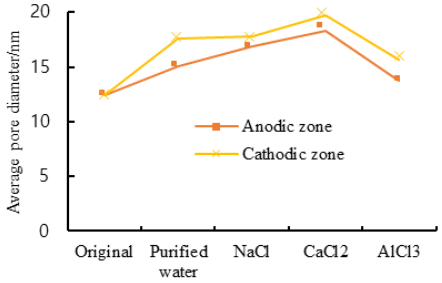

Fig. 7 Average pore diameter of modified specimens for different electrochemical aqueous solutions

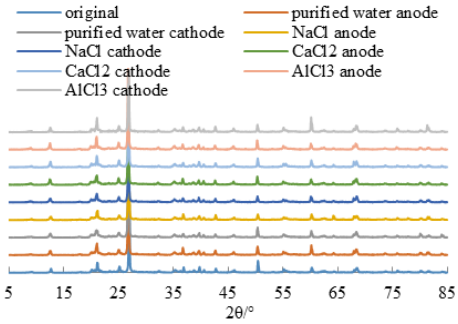

Fig. 8 X-ray diffraction patterns for specimens pre- and post-electrochemical modification

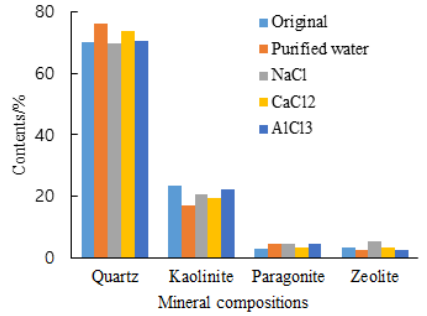

(a) Accumulated pore specific surface area

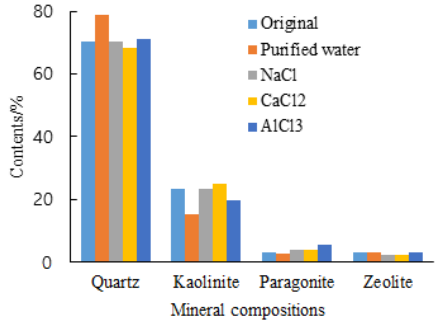

(b) Accumulated pore volume

Fig. 9 Mineral composition distribution in specimens pre- and post-electrochemical modification

3.5 UCS changes

The UCS was tested using a JL-WAW60 PC-controlled electro-hydraulic servo universal testing machine manufactured by Jilin Test Technology (Changchun, China),

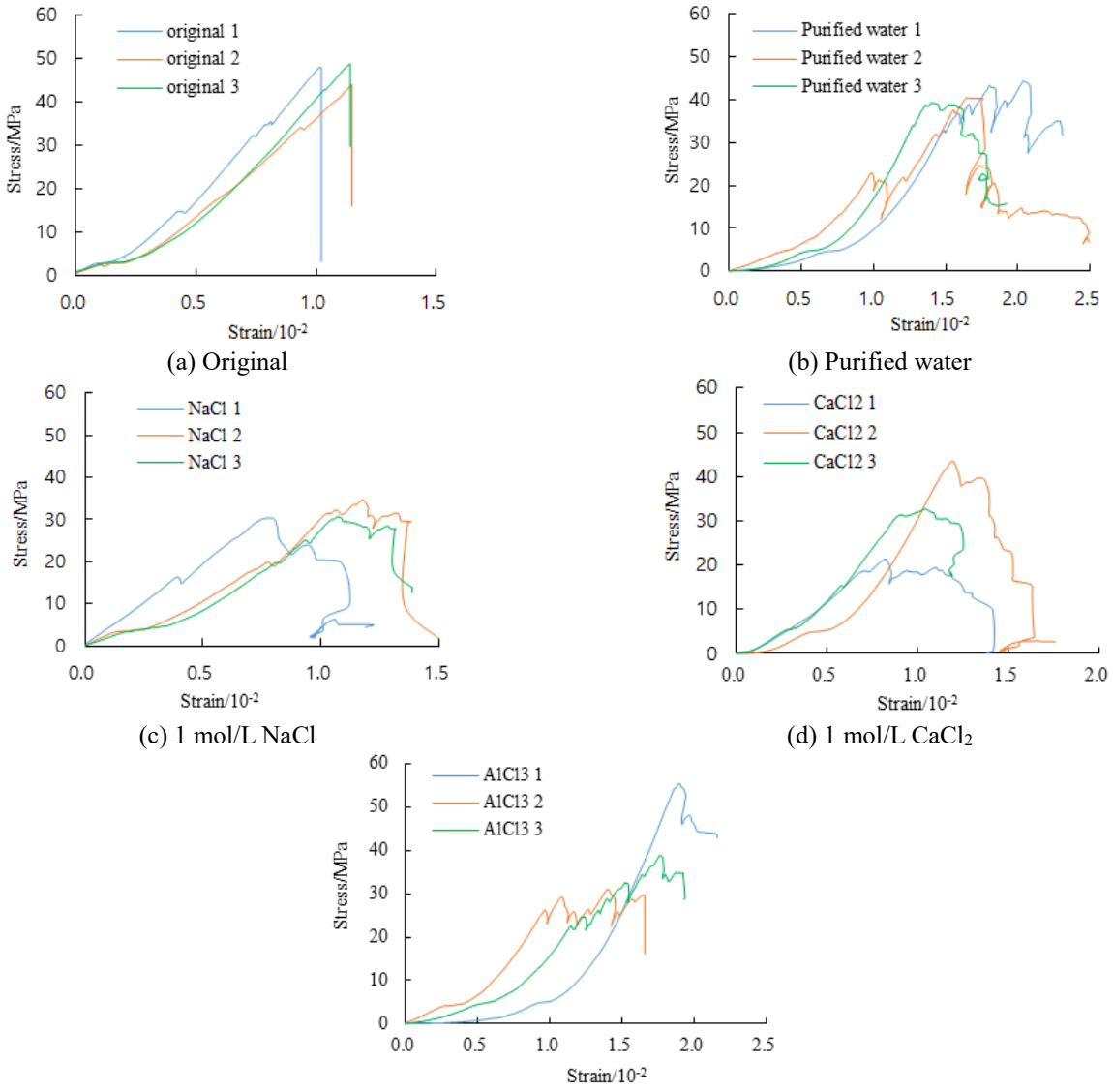

(a) Original

(b) Purified water

(c) 1 mol/L NaCl

(d) 1 mol/L $CaCl_2$

(e) 1 mol/L $AlCl_3$

Fig. 10 Stress-strain curves for modified specimens pre- and post-electrochemical modification

providing a maximum frame load capacity of 6.0×10^4 kg and a minimum displacement rate 1.0×10^{-3} mm/s, and servo-controlled variable loading rate. UCS tests were carried out in accordance with the ISRM suggested methods on each of the three samples in each group at a loading rate of 2.0×10^{-3} mm/s. Fig. 10 shows the complete stress-strain curves.

The following were observed:

(1) The UCS stress-strain curves for the original (unmodified) material were almost linear until failure, with no distinct yield point evident. After electrochemical modification the stress-strain curves were nonlinear to differing extents, with obvious yield points visible in all cases.

(2) The UCS of the modified samples was clearly much lower than the mean value of the original material (46.85 MPa), 40.77 MPa for purified water, 30.99 MPa for 1 mol/L NaCl, 32.53 MPa for 1 mol/L $CaCl_2$, and 41.69 MPa for 1 mol/L $AlCl_3$, representing reductions of 87.0%, 66.1%, 69.4% and 89.0% respectively. The UCS exactly followed the upward trend of the NaCl < $CaCl_2$ < purified water < $AlCl_3$, at 1 mol/L. But the progressive swelling of rock exactly is the opposite (Wakim et al 2009, Chai et al 2014), this trend is caused by the difference in swelling pressure between the interlayer space and the bulk solution (that is, the inner and outer solution). Swelling pressure is fundamentally related to the chemical potential and is directly associated with water activity. The water activity of 1 mol/L $AlCl_3$ is 0.939, smaller than 0.949 of 1 mol/L $CaCl_2$ and 0.967 of 1 mol/L NaCl, and this is why the UCS of rock trend is NaCl < $CaCl_2$ < purified water < $AlCl_3$, at 1 mol/L.

(3) The appearance of the stress-strain curves was changed from a single peak in the original material to multi-peak curves in the modified samples, evidently due to changes in the internal pore and fracture structures and an increasing number of flaws in the modified specimens. These defects fractured first, as the applied test load was increased up to the point of overall failure of the specimen. This is evident on the stress-strain curves as small strength reductions. The stress-strain curves in the post-failure

region show rapid strength decreases in varying stages, with small strength increases as the applied strain continued to be increased at a constant rate in the test. The small increases were due to transient frictional forces along the fracture surfaces of the collapsing specimen. (Such behavior is typical of the post-failure regime of rock materials.)

(4) The modified specimens exhibited plastic failure behavior, differing from the brittle failure behavior of the original material.

(5) For the $CaCl_2$ and $AlCl_3$ aqueous solutions, the differences of strength test date were greater than for the purified water and NaCl solution. This may have been caused by heterogeneity of corrosion and consequent weakening.

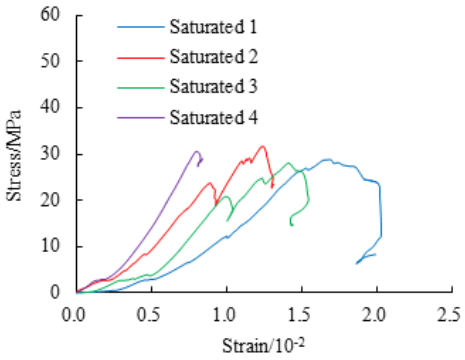

Fig. 11 Stress-strain curves of saturated rock samples

4. Discussion

(1) The electrodes were corroded during the electrochemical modification, mainly affecting the anode.

(2) Following electrochemical modification, the average pore diameter of the specimens increased and the accumulated pore specific surface area and volume both decreased. The accumulated pore specific surface area was greater in the anodic zone than the cathodic zone. The accumulated pore volume was less in the anodic zone than the cathodic zone.

(3) The UCS of the modified specimens was reduced markedly to between 66.1% and 89.0% of the value of the original specimen.

Regarding the observed corrosion of the electrodes (Figs. 2 and 3), Chew *et al.* (2004) carried out soft clay consolidation field trials using electric vertical drains, and Chai *et al.* (2016) reported a physical simulation of electrochemical modification of clayey rock. Applying a direct current to the specimen electrolyzes water molecules, altering the pH in the regions around the electrodes such that the acid (pH < 7) materials migrate towards the cathode, and the base (pH > 7) materials migrate towards the anode. The metal of the anodic electrode is corroded by oxidation in acidic conditions.

The variation in porosity before and after electrochemical modification was consistent with the results of Wang *et al.* (2010, 2011). The DC in the presence of the aqueous solutions stimulates the migration of electron, pore fluid, ions and fine particles through the matrix of the rock towards the oppositely charged electrode, thus creating the combined effects of a chemical, hydraulic and electrical (CHE) gradient. The pore fluid migrates from anode to cathode due to the capillary influence of the electric field. Negatively charged particles (usually micelles or colloids) agglomerate in the fluid stimulated by the electric gradient and coarsen in the anodic zone, tending to fill the pores and reduce porosity. The gradual movement of positive ions or positively charged electrical species in the presence of an electric gradient increases the degree of electro-osmosis and the electrolytic process, further increasing the porosity in the cathodic zone. This was confirmed by the laboratory test results in the present study.

The specimen UCS was altered by the electrochemical modification. Pinzari (1962) modified a mudstone core in coal measure rocks electrochemically, improving its tensile strength by a factor of 3.3. Chai *et al.* (2016), Lefebvre and Burnotte (2002), Shang *et al.* (2004) and Feijoo *et al.* (2017a, b) carried out electrochemical cementation laboratory and field tests in clayey rock, soft clays, calcareous soil and granite, respectively, and tested the mechanical strength of samples from the anodic zone, intermediate zone and cathodic zone of the treated specimens. They all found that the trend of the strength was anode > intermediate > cathode for all samples. An XRD and micro computed tomography study by Wang *et al.* (2011) of the variation in mineralogical composition and pore structure of mudstone after electrochemical modification indicated that new minerals were created, porosity decreased and the strength of the mudstone was altered. Studies by Sousa *et al.* (2005) and Dagdelenler *et al.* (2011) found that greater porosity lowered the strength of the test material, especially the UCS, because the presence of the additional pores reduces the bearing cross-sectional area of the skeleton of the test specimen, and the pores act as stress concentrators.

The following two aspects contribute to reduction in test specimen strength:

(1) The difference in moisture content of test specimens. The moisture content of the original (unmodified) specimens is the natural value, but is close to saturation during the electrochemical modification process. Increasing the moisture content is known to sharply reduce the UCS and elastic modulus and increase the Poisson's ratio of sandstone (Li *et al.* 2017, Szewczyk *et al.* 2017, Huang *et al.* 2018, Salih and Mohanned 2017). Fig. 11 illustrates the uniaxial compressive stress-strain curves of saturated rock sample. The uniaxial compressive strength were 28.87MPa, 31.64MPa, 28.11MPa and 30.52MPa, respectively. Average 29.79MPa, which was only 63.6% of the uniaxial compressive strength of original samples, 46.85MPa.

(2) The corrosive and weakening effects of the aqueous solution on sandstone (Feng *et al.* 2004, Gao and Ge 2016). The aqueous solution leaching process activates migration and dissolution of rock grains in sandstone due to the reactions between H^+ in the liquid and the active minerals. This produces new micro-pores, which gradually increase in size due to the erosive and electrokinetic effects induced by the combined electric, hydraulic and chemical coupling. This leads to the generation and development of new pores, further increasing the heterogeneity of the rock and

reducing the connective and frictional forces between particles.

Since mineralogical composition of specimens little or no contain soluble minerals, the moisture content is the more important factors contributed to the reduction of specimen strength. In practive, strip out the impact of difference in moisture content of test specimens, and the specimen UCS was increased to varying degrees by the electrochemical modification. 1.37 times for pruified water, 1.04 times for 1 mol/L NaCl, 1.09 times for 1 mol/L $CaCl_2$, and 1.40 times for 1 mol/L $AlCl_3$, respectively.

5. Conclusions

An experimental study was conducted to assess the electrochemical modification of sandstone sampled from Paleozoic coal measure strata located in central China. The study focused on the changes to the physical and mechanical properties of the rock. The results are summarized as follows.

• In general, modification with a direct electric current generates electrokinetic phenomena (mainly electro-migration/ion migration, electrophoresis and electro-osmosis) which affect the pores in the sandstone fabric and alter the pore structure of the material.

• The average pore size in the modified rock was found to have increased, and the porosity (number of pores) decreased. The accumulated pore specific surface area in the anodic zone of the samples was greater than in the cathodic zone. The accumulated pore volume in the anodic zone was less than in the cathodic zone.

• The mineralogical composition of specimens was examined following modification and found to be unchanged.

• The change in strength of the sandstone was an artifact of the combined effect of electrochemical cementation and aqueous chemical corrosion, and electrochemical cementation stronger than aqueous chemical corrosion.

Acknowledgements

This work was supported by the National Natural Science Foundation of China, grants no. 51004075 and 51674173, by Shanxi Province Science Foundation, grant no. 201601D102038, by the Shanxi Scholarship Council of China, grant no. 2016-040, and by the Shanxi Province Key Research and Development program (international cooperation and exchange), grant No. 201803D421078.

References

Aggour, M.A. and Muhammadain, A.M. (1992), "Investigation of water-flooding under the effect of electrical potential gradient", *J. Petrol. Sci. Eng.*, **7**(3/4), 319-327

Aggour, M.A., Tchelepi, H.A. and Yousef, H.Y. (1994), "Effect of electroosmosis on relative permeability of sandstones", *J. Petrol. Sci. Eng.*, **11**(2), 91-102.

Bernabeu, A., Expósito, E., Montiel, V., Ordóñez, S. and Aldaz, A. (2001), "A new electrochemical method for consolidation of porous rocks", *Electrochem. Commun.*, **3**(3), 122-127.

Casagrande, L. (1952), "Electro-osmotic stabilization of soils", *J. Boston Soc. Civ. Eng.*, **39**(1), 51-83

Chai, Z., Kang, T. and Feng, G. (2014), "Effect of aqueous solution chemistry on the swelling of clayey rock", *Appl. Clay Sci.*, **93**, 12-16

Chai, Z., Zhang, Y. and Alexander, S. (2016), "Study of physical simulation of electrochemical modification of clayey rock", *Geomech. Eng.*, **11**(2), 197-209

Chew, S.H., Karumaratne, G.P., Kuma, V.M., Lim, L.H., Toh, M.L. and Hee, A.M. (2004), "A field trial for soft clay consolidation using electric vertical drains", *Geotext. Geomembranes*, **22**(1-2), 17-35

Chilingar, G. (1970), "Effect of direct electrical current on permeability of sandstone cores", *J. Petrol. Technol.*, **22**(7), 8-17.

Dagdelenler, G., Sezer, E.A. and Gokceoglu, C. (2011), "Some non-linear models to predict the weathering degrees of a granitic rock from physical and mechanical parameters", *Expert Syst. Appl.*, **38**(6), 7476-7485

Feijoo, J., Ottosen, L.M., Nóvoa, X.R. Rivas, T and Rosaril, I.D (2017a), "An improved electrokinetic method to consolidate porous materials", *Mater. Struct.*, **50**(3), 186

Feijoo, J., Nóvoa, X.R. and Rivas, T. (2017b), "Electrokinetic treatment to increase bearing capacity and durability of a granite", *Mater. Struct.*, **50**(6), 251

Feijoo, J., Rivas, T., Nóvoa, X.R., Rosaril, I.D and Oterro, J. (2018), "In situ desalination of a granitic column by the electrkinetic method", *Int. J. Architect. Heritage*, **12**(1), 63-74

Feng, X., Chen, S. and Zhou, H. (2004), "Real-time computerized tomography (CT) experiments on sandstone damage evolution during triaxial compression with chemical corrosion", *Int. J. Rock Mech. Min. Sci.*, **41**(2), 181-192

Gao, W and Ge, M. (2016), "Fracture of rock affected by chemical erosion environment", *Geomech. Eng.*, **11**(3), 373-383

Huang, Y., Yang, S., Matthew, R.H. and Zhang. Y. (2018), "The effects of NaCl concentration and confining pressure on mechanical and acoustic behaviors of brine-saturated sandstone", *Energies*, **11**(2), 385

Lefebvre, G. and Burnotte, F. (2002), "Improvements of electro-osmotic consolidation of soft clays by minimizing power loss at electrodes", *Can. Geotech. J.*, **39**(2), 399-408

Li, G., Qi, C., Sun, Y., Tang, X. and Hou, B. (2017), "Experimental study on the softening characteristics of sandstone and mudstone in relation to moisture content", *Shock Vib.*, (6), 1-14

Pinzari, U. (1962), "Indagine sul trattamento elettrosmotico di un materiale argilloso", *Geotecnica*, **9**(3), 101-114.

Salih, N. and Mohammed, A. (2017), "Characterization and modeling of long-term stress-strain behavior of water confined pre-saturated gypsum rock in kurdistan region, Iraq", *J. Rock Mech. Geotech. Eng.*, **9**(4),741-748

Shang J., Mohamedelhassan, E. and Ismail, M. (2004), "Electrochemical cementation of offshore calcareous soil", *Can. Geotech. J.*, **41**(5), 877-893

Sousa, L.M.O., Suárez del Río, L.M., Calleja, L., Ruiz de Argandoña, V.G. and Rodríguez Rey, A. (2005), "Influence of microfractures and porosity on the physicomechanical properties and weathering of ornamental granites", *Eng. Geol.*, **77**(1), 153-168.

Szewczyk, D., Holt, R.M. and Bauer, A. (2017), "The impact of saturation on seismic dispersion in shales-laboratory measurements", *Geophysics*, **83**(1), 15-34

Wakim, J., Hadj-Hassen, F. and Windt, L.D. (2009), "Effect of aqueous solution chemistry on the swelling and shrinkage of the Tournemire shale", *Int. J. Rock Mech. Min. Sci.*, **46**(8), 1378-1382

Wang, D., Kang, T., Han, W., Liu, Z. and Chai, Z. (2010), "Electrochemical modification of the porosity and zeta potential of montmorillonitic soft rock", *Geomech*. *Eng*., **2**(3), 191-202
Wang, D., Kang, T., Han, W. and Liu, Z. (2011), "Electrochemical modification of tensile strength and pore structure in mudstone", *Int*. *J*. *Rock Mech*. *Min*. *Sci*., **48**(4), 687-692

CC